Refined and generalized hybrid type quasi-3D shear deformation theory for the bending analysis of functionally graded shells

J.L. Mantari

[+]Universidad de Ingeniería y Tecnología, Av. Cascanueces 2221, Santa Anita, Lima, Perú.

Abstract. The closed-form solution of a generalized hybrid type quasi-3D higher order shear deformation theory (HSDT) for the bending analysis of functionally graded shells is presented. From the generalized quasi-3D HSDT (which involves the shear strain functions "$f(\zeta)$" and "$g(\zeta)$" and therefore their parameters to be selected "m" and "n", respectively), infinite six unknowns' hybrid shear deformation theories with thickness stretching effect included, can be derived and solved in a closed-from. The generalized governing equations are also "m" and "n" parameter dependent. Navier-type closed-form solution is obtained for functionally graded shells subjected to transverse load for simply supported boundary conditions. Numerical results of new optimized hybrid type quasi-3D HSDTs are compared with the first order shear deformation theory (FSDT), and other quasi-3D HSDTs. The key conclusions that emerge from the present numerical results suggest that: (a) all non-polynomial HSDTs should be optimized in order to improve the accuracy of those theories; (b) the optimization procedure in all the cases is, in general, beneficial in terms of accuracy of the non-polynomial hybrid type quasi-3D HSDT; (c) it is possible to gain accuracy by keeping the unknowns constant; (d) there is not unique quasi-3D HSDT which performs well in any particular example problems, i.e. there exists a problem dependency matter.

---

[1]Corresponding Author email: jmantari@utec.edu.pe Tel: +00511 3540070; Cell: +0051 962224551;

Keywords: A. Plates; B. Elasticity; C. Analytical modeling

1. Introduction

Laminated composite structures such as shells are extensively used in the industry. However, even the designer's effort to tailor different laminate properties to suit a particular application; some laminated composite structures suffer from discontinuity of material properties at the interface of the layers and constituents of the composite. Therefore the stress fields in these regions create interface problems and thermal stress concentrations under high temperature environments. Furthermore, large plastic deformation of the interface may trigger the initiation and propagation of cracks in the material [1]. In order to alleviate this problem, functionally graded materials (FGMs) were proposed by Bever and Duwez [2]. Then, this kind of materials were developed and successfully used in industrial applications since 1984 [3].

In the most general case, FGMs are materials with spatial variation of the material properties. However, in most of the applications reported in the literature, as in the present work, the variation is only along the thickness; demonstrating the present state of development of FGMs.

Recently, several researchers have reported results on functionally graded plates (FGPs) and shells. Both analytical and numerical solutions for these cases can be found in the literature, Birman and Byrd [4], see also Mantari and Guedes Soares [5-9]. An updated literature review of FGMs can be found in the work by Jha et al. [10]. In the present article, the relevant and recent related work on functionally graded shells is described in what follows.

Readers interested in developing HSDTs should consult the referential papers by Reddy [11], Vel and Batra [12-13] and Cheng and Batra [14]. Alternative bibliografy can be also the paper by Liew et al [15] on postbuckling analysis of functionally graded cylindrical shells under axial compression and thermal loads using the element-free kp-Ritz method. In this paper, the authors developed the formulation to handle problems of small strains and moderate rotations, based on the FSDT for shells and von Kármán strains.

Sofiyev and Kuruoglu [16] studied the torsional vibration and buckling of cylindrical shells with FG coatings surrounded by an elastic medium. Consequently, Sofiyev and Kuruoglu [17] presented a theoretical approach to solve vibration problems of FG truncated conical shells under mixed boundary conditions. Then, Sofiyev [18] investigated the dynamic instability of exponentially graded sandwich cylindrical shells under static and time dependent periodic axial loadings using HSDT.

Deniz [19] studied the response of a FG coated truncated conical shell subjected to an axial load. The author performed the analysis through non-linear equations governing the finite deformations of the shell. Ghannad et al. [20] presented an analytical solution for deformations and stresses of axisymmetric clamped–clamped thick cylindrical shells with variable thickness made of FGMs subjected to internal pressure. The authors used the FSDT and matched asymptotic method (MAM) of the perturbation theory.

Fraldi and colleagues [21] presented the exact analytical solutions for the elastic response of a solid circular cylinder composed by the assembly of a central core and *n* surrounding hollow phases, all made of different homogeneous elastic materials, under de Saint Venant load conditions. The authors obtained an equivalent one-dimensional homogenized beam model for the whole object. Tornabene et al. [22] performed an extensive study on doubly-curved FG shells structures using CUF and the Murakami's Zig-Zag (ZZ) function. The authors used the Generalized Differential Quadrature (GDQ) method and good referential results were obtained.

Xie et al. [23] used the Haar Wavelet Discretization (HWD) method-based solution approach to study the free vibration analysis of FG spherical and parabolic shells of revolution with arbitrary boundary conditions along with the FSDT. Kim [24] studied the free vibration characteristics of FG cylindrical shells partially resting on elastic foundation with an oblique edge by using the FSDT. Shooshtari and Razavi [25] studied, analytically and by using the FSDT, the linear and nonlinear free vibration of symmetrically laminated magneto-electro-elastic doubly-curved thin shell resting on an elastic foundation. Qu et al. [26] described a general formulation for free, steady-state and transient vibration analyses of FG shells of revolution subjected to arbitrary boundary conditions. The formulation is derived by means of a modified variational principle in conjunction with a multi-segment partitioning procedure on the basis of the FSDT. Thai

and Kim [27] performed a remarkable review on equivalent single layer theories (ESL) in the modelling of functionally graded plates and shells.

Carrera and co-workers [28] studied the static analysis of FGPs and shells. The stretching effect was included in the mathematical formulation and the importance of the transverse normal strain effects in the mechanical prediction of stresses of FGPs and shells was remarked. Neves et al. [29][30] and Ferreira et al. [31] presented a quasi-3D hybrid type (polynomial and trigonometric) shear deformation theory for the static and free vibration analysis of functionally graded plates by using meshless numerical method. Their formulation can be seen as a generalization of the original Carreras's Unified Formulation (CUF), by introducing different non-polynomial displacement fields for in-plane displacements, and polynomial displacement field for the out-of-plane displacement. Mantari and Guedes Soares [5-9] presented bending results of FGM by using new non-polynomial HSDTs. In [7] and [8], the stretching effect was included and improved results of displacement and in plane normal stresses compared with [5] and [6] were found. Recently, the authors developed an accurate and attractive optimized quasi-3D HSDTs for advanced composite plates and shells [32][33] by utilizing the well-known polynomial sinusoidal shear strain shape function.

In the other hand, on the basis of the 4-unknown plate theory and polynomial shear strain shape function, Abdelaziz et al. [34] studied the static analysis of FG sandwich plates. Consequently, Mechab et al. [35] considered the static and dynamic analysis of FGPs with new non-polynomial shear strain shape function (hyperbolic). Recently, a 5 unknown variables trigonometric plate theory (TPT) with stretching effect was developed by Thai and Kim [36] showing good accuracy with respect to its counterpart the TPT with 6-unknows.

Looking for generalized formulations of shear deformation theories for classical and advanced composites, it can be said that they are rare in the literature. Regarding to generalized formulations in classical composites, it is important to remark the work done by Soldatos [37], Carrera (CUF) [38] and Demasi [39,40], Mantari and Guedes Soares [41].

Besides the powerful CUF there exists a generalized formulation proposed by Zenkour [42], which were extended to cover the stretching effect in Zenkour [43].

Matusanga [44] also developed a generalized HSDT based on polynomial shear strain shape functions. In Mantari and Guedes Soares [8], a generalized hybrid type HSDT for plates was developed. This generalized theory is able to reproduce the theory proposed in [7][43] and others as special case.

The generalized HSDT of functionally graded plates presented by Zenkour [42][43] is similar to the one formulated by Soldatos [37] for laminated composites. Normally non-polynomial share strain shape functions, such as trigonometric, trigonometric hyperbolic, exponential, etc., can be used in this type of generalized formulation, see also Mantari and Guedes Soares [41]. However, the thickness expansion model ($g(z)$) is conditioned by the in-plane displacement model ($f(z)$), i.e. the transverse shear strain function is an even function which is the derivative of the in-plane shear strain shape function ($g(z) = f'(z)$). Therefore, there is no freedom in choosing the shear strain shape functions, i.e. the through the thickness displacement field modeling.

The present formulation has that freedom, i.e. $g(z)$ can be $f'(z)$ or different transverse shear strain function, and therefore infinite hybrid type shear deformation theories (polynomial or non-polynomial or hybrid type) can be created just having 6 unknown variables or 6 degree of freedom (DOF) for finite element analysis.

The generalized hybrid type HSDT for plates and shells presented here, and for example the well-known CUF (extended to include non-polynomial shape strain functions in their formulation [29-31]) demand the development of new non-polynomial shape strain functions, which can be adapted to this advanced generalized formulation perhaps for better performance. In the present work, in addition to the main contribution of the present paper, new non-polynomial shape strain functions are presented for the first time.

It is important to remark that the static or bending problem of *shells* made of FGMs are not much explored neither available in the literature with the exception of CPT formulations (in the case of *plate* bending problems based on shear deformation theories, the contribution is quite representative), it may be because not much attention were given to the static behavior of FGMs compared with thermomechanical behavior which initially was the main concern due to the application requirements. Moreover, the non-polynomial function based-HSDTs are not widely used compared with the polynomial function

based-HSDTs except for the case of the sinusoidal shear deformation theory (SSDT) as reported by Thai and Kim [27] who performed an interesting review on shells and functionally graded materials in the context of equivalent single layer and PVD and RMVT variational statements. In both directions, this paper contributes with the implementation of new quasi-3D non-polynomial hybrid type HSDTs to study the bending problem of single and sandwich shells. The SSDT with 5 and 6 unknown variables were previously optimized by this author and Guedes Soares [32-33]. In ref. [32] the bending shell problem were studied through elegant optimized SSDT.

In this paper a generalized quasi-3D hybrid type HSDT for shells having fixed number of unknowns, 6 in this case, is formulated and can be further optimized depending on the free selection of the shear strain shape functions. Moreover, several new quasi-3D hybrid type HSDTs were optimized and introduced to study the bending problems of shells using non-polynomial HSDTs which are rare in the literature. The generalized theory complies with the tangential stress-free boundary conditions on the plate boundary surface, and thus a shear correction factor is not required. The plate governing equations and its boundary conditions are derived by employing the principle of virtual work. Navier-type analytical solutions are obtained for shells subjected to transverse load for simply supported boundary conditions. Benchmark results for the displacement and stresses of functionally graded rectangular plates are obtained. The results of some new hybrid HSDTs are compared with 3D exact, quasi-exact, and with other closed-form solutions published in the literature.

2. Theoretical Formulation

The rectangular doubly-curved shell made of FGM of uniform thickness, h, is shown in Figure 1. The ξ_1 and ξ_2 curves are lines of curvature on the shell mid-surface, $\xi_3 = \zeta = 0$, while $\xi_3 = \zeta$ is a straight line normal to the mid-surface. The principal radii of normal curvature of the reference (middle) surface are denoted by R_1 and R_2. The generalized displacement field satisfying the conditions of transverse shear stresses (and

hence strains) vanishing at a point (ξ_1, ξ_2, $\pm h/2$) on the outer (top) and inner (bottom) surfaces of the shell, is given as follows:

$$\bar{u} = (1+\frac{\zeta}{R_1})u + \zeta\left[y^* \theta_1 + q^* \frac{\partial \theta_3}{a_1 \partial x} - \frac{\partial w}{a_1 \partial x} \right] + f(\zeta)\theta_1,$$

$$\bar{v} = (1+\frac{\zeta}{R_2})v + \zeta\left[y^* \theta_2 + q^* \frac{\partial \theta_3}{a_2 \partial y} - \frac{\partial w}{a_2 \partial y} \right] + f(\zeta)\theta_2,$$

$$\bar{w} = w + g(\zeta)\theta_3, \qquad \text{(1a-c)}$$

where $\mathrm{u}(\xi_1,\xi_2)$, $\mathrm{v}(\xi_1,\xi_2)$ and $\mathrm{w}(\xi_1,\xi_2)$ are the mid-plane displacements; $\Theta_1(\xi_1,\xi_2)$, $\Theta_2(\xi_1,\xi_2)$ and $\Theta_3(\xi_1,\xi_2)$ are rotations of normal to the mid-plane about ξ_2-, ξ_1- and ξ_3-axis. They are the six unknown displacement functions of the middle surface of the panel (6 DOFs), while $y^* = -f'(\frac{h}{2})$ and $q^* = -g(\frac{h}{2})$ (being h the thickness of the shell), a_1 and a_2 are scalar values inherent to the type of shells. These scalar values are associated to the vectors tangent to the ξ_1 and ξ_2 coordinate lines, respectively, for more details readers may consult the interesting book written by Reddy [45]. The theory allows the inclusion of a freely chosen shear strain shape function, $f(z)$ (odd function), and $g(z)$ (even).

In the derivation of the necessary equations, small elastic deformations are assumed, i.e. displacements and rotations are small, and obey Hooke's law. The starting point of the present thick shell theory is the 3D elasticity theory [45], expressed in general curvilinear (reference) surface-parallel coordinates; while the thickness coordinate is normal to the reference (middle) surface as given in Figure 1.

Replacing the Equations (1a-c) into the elasticity equations [45] (see Appendix A) for a moderately shallow and deep shell, the following strain-displacement relations, valid for a doubly-curved panel under consideration can be obtained:

$$\varepsilon_{xx} = \varepsilon^0_{xx} + \zeta\varepsilon^1_{xx} + f(\zeta)\varepsilon^2_{xx},$$

$$\varepsilon_{yy} = \varepsilon^0_{yy} + \zeta\varepsilon^1_{yy} + f(\zeta)\varepsilon^2_{yy},$$

$$\varepsilon_{zz} = g'(\zeta)\varepsilon^5_{zz},$$

$$\varepsilon_{yz} = \varepsilon_{yz}^{0} + g(\zeta)\varepsilon_{yz}^{3} + f'(\zeta)\varepsilon_{yz}^{4},$$

$$\varepsilon_{xz} = \varepsilon_{xz}^{0} + g(\zeta)\varepsilon_{xz}^{3} + f'(\zeta)\varepsilon_{xz}^{4},$$

$$\varepsilon_{xy} = \varepsilon_{xy}^{0} + \zeta\varepsilon_{xy}^{1} + f(\zeta)\varepsilon_{xy}^{2}. \qquad \text{(2a-f)}$$

An FG shell of length *a*, width *b* and a total thickness *h* made of a mixture of metal and ceramic materials are considered in the present analysis. The elastic material properties vary through the thickness and the power-law distribution is assumed to describe the variation of material properties, which is expressed as

$$P(\zeta) = \begin{cases} VP_b, \quad V = e^{p\left(\frac{\zeta}{h}+\frac{1}{2}\right)}, \text{ for } \exp \text{onentially graded shells}. \\ (P_t - P_b)V + P_b, \quad V = \left(\frac{\zeta}{h}+\frac{1}{2}\right)^{p}, \text{ for functionally graded shells } (\textit{mixture rule}). \end{cases} \qquad \text{(3a-b)}$$

where P denotes the effective material property, P_t and P_b denote the property of the top and bottom faces of the panel, respectively, and p is the power-law exponent that specifies the material variation profile through the thickness. The effective material properties of the shell, including Young's modulus, E and shear modulus, G vary according to Equations (3a-b), and the Poisson ratio, ν is assumed to be constant.

Considering the static version of the principle of virtual work and the stress-strain relationship through hook's law, the following expressions can be obtained:

$$0 = \left[\int_{-h/2}^{h/2} \left\{ \int_{\Omega} \left[\sigma_{xx}^{(k)}\delta\varepsilon_{xx} + \sigma_{yy}^{(k)}\delta\varepsilon_{yy} + \sigma_{zz}^{(k)}\delta\varepsilon_{zz} + \sigma_{yz}^{(k)}\delta\varepsilon_{yz} + \sigma_{xz}^{(k)}\delta\varepsilon_{xz} + \sigma_{xy}^{(k)}\delta\varepsilon_{xy} \right] dxdy \right\} d\zeta \right]$$

$$- \left[\int_{\Omega} q\delta\bar{w} dxdy \right], \qquad \text{(4)}$$

$$0 = \int_{\Omega} (N_1\delta\varepsilon_{xx}^{0} + M_1\delta\varepsilon_{xx}^{1} + P_1\delta\varepsilon_{xx}^{2} + N_2\delta\varepsilon_{yy}^{0} + M_2\delta\varepsilon_{yy}^{1} + P_2\delta\varepsilon_{yy}^{2} + R_3\delta\varepsilon_{zz}^{4} + N_4\delta\varepsilon_{yz}^{0} + Q_4\delta\varepsilon_{yz}^{3} +$$

$$K_4\delta\varepsilon_{yz}^{4} + N_5\delta\varepsilon_{xz}^{0} + Q_5\delta\varepsilon_{xz}^{3} + K_5\delta\varepsilon_{xz}^{4} + N_6\delta\varepsilon_{xy}^{0} + M_6\delta\varepsilon_{xy}^{1} + P_6\delta\varepsilon_{xy}^{2} - q\delta\bar{w}) dxdy. \qquad \text{(5)}$$

where $\varepsilon^{(k)}$ or $\sigma^{(k)}$ are the stresses and the strain vectors of the k[th] layer, q is the distributed transverse load; and N_i, M_i, P_i, Q_i and K_i are the resultants of the following integrations:

$$(N_i, M_i, P_i) = \sum_{k=1}^{N} \int_{z^{(k-1)}}^{z^{(k)}} \sigma_{i(\zeta)}^{(k)} (1, \zeta, f(\zeta)) d\zeta, \qquad \text{(i=1, 2, 6)}$$

$$N_i = \sum_{k=1}^{N} \int_{z^{(k-1)}}^{z^{(k)}} \sigma_{i(\zeta)}^{(k)} d\zeta, \qquad \text{(i=4, 5)}$$

$$(Q_i, K_i) = \sum_{k=1}^{N} \int_{z^{(k-1)}}^{z^{(k)}} \sigma_{i(\zeta)}^{(k)} (g(\zeta), f'(\zeta)) d\zeta, \qquad \text{(i=4, 5)}$$

$$R_i = \sum_{k=1}^{N} \int_{z^{(k-1)}}^{z^{(k)}} \sigma_{i(\zeta)}^{(k)} g'(\zeta) d\zeta. \qquad \text{(i=3)} \qquad \text{(6a-d)}$$

The generalized static version of the governing equations are derived from Equation (5) by integrating by parts the displacement gradients and setting the coefficients of $\delta u, \delta v, \delta w, \delta\theta_1, \delta\theta_2$ and $\delta\theta_3$ to zero separately. The generalized equations obtained are as follows:

$$\delta u: \frac{\partial M_1}{R_1 \partial x_1} + \frac{\partial M_6}{R_1 \partial x_2} + \frac{\partial N_1}{\partial x_1} + \frac{\partial N_6}{\partial x_2} = 0,$$

$$\delta v: \frac{\partial M_2}{R_2 \partial x_2} + \frac{\partial M_6}{R_2 \partial x_1} + \frac{\partial N_2}{\partial x_2} + \frac{\partial N_6}{\partial x_1} = 0,$$

$$\delta w: -\frac{N_1}{R_1} - \frac{N_2}{R_2} + \frac{\partial^2 M_1}{\partial x_1^2} + \frac{\partial^2 M_2}{\partial x_2^2} + 2\frac{\partial^2 M_6}{\partial x_1 \partial x_2} + q = 0,$$

$$\delta\theta_1: y^*\left(\frac{\partial M_1}{\partial x_1} + \frac{\partial M_6}{\partial x_2} - N_5\right) + \frac{\partial P_1}{\partial x_1} + \frac{\partial P_6}{\partial x_2} - K_5 = 0,$$

$$\delta\theta_2: y^*\left(\frac{\partial M_2}{\partial x_2} + \frac{\partial M_6}{\partial x_1} - N_4\right) + \frac{\partial P_2}{\partial x_2} + \frac{\partial P_6}{\partial x_1} - K_4 = 0,$$

$$\delta\theta_3 : -\frac{Q_1}{R_1} - \frac{Q_2}{R_2} + q^*\left(\frac{\partial N_4}{\partial x_2} + \frac{\partial N_5}{\partial x_1} - \frac{\partial^2 M_1}{\partial x_1^{\,2}} - \frac{\partial^2 M_2}{\partial x_2^{\,2}} - 2\frac{\partial^2 M_6}{\partial x_1 \partial x_2}\right) + \frac{\partial Q_4}{\partial x_2} + \frac{\partial Q_5}{\partial x_1} - R_3 - q^* q = 0 .$$

(7a-f)

In what follows, the problem under consideration is solved for the following simply supported boundary conditions prescribed at all four edges:

$N_1 = M_1 = P_1 = v = w = \theta_2 = \theta_3$ at x = 0, a,

$N_2 = M_2 = P_2 = u = w = \theta_1 = \theta_3$ at y = 0, b. (8a-b)

3. Solution procedure

Exact solutions of the generalized partial differential equations (7a-f) on arbitrary domain and for general boundary conditions are difficult to find. Although the Navier type solutions can be used to validate the present theory, more general boundary conditions will require solution strategies involving, e.g. boundary discontinuous double Fourier series approach (see for example Oktem and Guedes Soares [46]).

Solution functions that completely satisfy the boundary conditions in Equations (8a-b) are assumed as follows:

$$u(x,y) = \sum_{r=1}^{\infty}\sum_{s=1}^{\infty} U_{rs}\cos(\alpha x)\sin(\beta y), \qquad 0 \le x \le a;\ 0 \le y \le b$$

$$v(x,y) = \sum_{r=1}^{\infty}\sum_{s=1}^{\infty} V_{rs}\sin(\alpha x)\cos(\beta y), \qquad 0 \le x \le a;\ 0 \le y \le b$$

$$w(x,y) = \sum_{r=1}^{\infty}\sum_{s=1}^{\infty} W_{rs}\sin(\alpha x)\sin(\beta y), \qquad 0 \le x \le a;\ 0 \le y \le b$$

$$\theta_1(x,y) = \sum_{r=1}^{\infty}\sum_{s=1}^{\infty} \theta_{rs}^{1}\cos(\alpha x)\sin(\beta y), \qquad 0 \le x \le a;\ 0 \le y \le b$$

$$\theta_2(x,y) = \sum_{r=1}^{\infty}\sum_{s=1}^{\infty} \theta_{rs}^{2}\sin(\alpha x)\cos(\beta y), \qquad 0 \le x \le a;\ 0 \le y \le b$$

$$\theta_3(x,y) = \sum_{r=1}^{\infty}\sum_{s=1}^{\infty} \theta_{rs}^{3}\sin(\alpha x)\sin(\beta y), \qquad 0 \le x \le a;\ 0 \le y \le b$$

(9a-f)

where

$$\alpha = \frac{r\pi}{a},\ \beta = \frac{s\pi}{b}. \tag{10}$$

Substituting Equations (9a-f) into Equations (7a-f), the following equations are obtained,

$$K_{ij} d_j = F_j \qquad (i, j = 1,.....,6) \text{ and } (K_{ij} = K_{ji}). \tag{11}$$

Elements of K_{ij} in Equation (11) can be obtained by using Ref. [32] and the governing equations 12(a-f).

$$\{d_j\}^T = \{U_{rs} \ \ V_{rs} \ \ W_{rs} \ \ \Theta^1_{rs} \ \ \Theta^2_{rs} \ \ \Theta^3_{rs}\}, \tag{12}$$

$$\{F_j\}^T = \{0 \ \ 0 \ \ Q_{rs} \ \ 0 \ \ 0 \ \ -q^* Q_{rs}\} \tag{13}$$

where Q_{rs} are the coefficients in the double Fourier expansion of the transverse load,

$$q(x, y) = \sum_{r=1}^{\infty} \sum_{s=1}^{\infty} Q_{rs} \sin(\alpha x) \sin(\beta y). \tag{14}$$

4. Numerical Results and Discussion

In the present section, the results of the bending analyses of FG plates and shells are presented. The results were obtained from the present generalized hybrid type quasi-3D HSDTs with new shear strain shape functions. The theory is formulated in such way that the thickness stretching effect (TSE) can be taken into account, i.e. the thickness expansion is well-modelled by obeying the Koiter's recommendation [47], for further information the reader is referred to Carrera et al. [28].

The main aim of the present paper is to develop an unavailable generalized hybrid-quasi-3D HSDT for shells. However, new and well-known optimized shear strain functions are also presented. In addition, the foundations to obtain very accurate shear strain functions which can allow finding accurate HSDTs are given. The "*problem dependency matter*" regarding to the precision of HSDTs is noticed and discussed for advanced composites. Based on the optimization procedure given in this paper, future works may be conducted in order to find out the most accurate HSDT having a limited number of unknown variables for classical and advanced composite plates.

Four pairs of shear strain functions ($f(\zeta)$ and $g(\zeta)$) are studied in the context of the present generalized theory, so four different quasi-3D HSDTs are obtained. The first HSDT is the well-known trigonometric plate theory TPT (HSDT1) which was here optimized for advanced composite plates. The second one is the new tangential trigonometric HSDT. The third one is the hybrid type HSDT which combines trigonometric and exponential shear strain functions. The fourth one is the polynomial quasi-3D HSDT. Table 1 presents more details regarding the shear strain function used in this paper. It should keep in mind that the shear strain shape functions presented in Table 1 allow the transverse shear deformation to have an approximately parabolic distribution and it satisfies exactly the zero shear stress conditions on the upper and lower plate surfaces. It is also important to mention that this generalized formulation avoid the use of complex shear strain function expressions as when accurate 5 unknown HSDTs without TSE are looked for, see for example Mantari and Guedes Soares [41].

In this paper, in fact, the options to select the shear strain shape functions can be infinite and as simple as polynomial HSDT or other more accurate non-polynomial functions, and also hybrid type (see Table 1) can be utilized.

The selection of the unknown parameter "*m*" and "*n*" of the shear strain shape functions belonging to each quasi-3D HSDTs presented in Table 1 are discussed in what follows. Additionally, results reproduced by the present generalized hybrid type quasi-3D HSDT are compared with the exact solution provided by Zenkour [43] and other HSDTs available in the literature.

4.1 Selection of the parameters "*m*" and "*n*" of the shear strain shape functions "*f*(ζ)" and "*g*(ζ)"

The generalized displacement field in Equations 1a-c are formulated with "*f*(ζ)" and "*g*(ζ)" and therefore with "*m*" and "*n*" parameter dependency (see Table 1). The generalized governing equations (Equations 12a-f) are formulated with "y^*" and "q^*", and therefore they are also "*m*" and "*n*" parameter dependent (see Table 1). The unknown parameter "*m*" and "*n*" of each of the HSDTs presented in Table 1 are obtained by providing: (a) the center plate deflection, $\bar{w}$(a/2, b/2, 0); and (b) the inplane normal stresses $\bar{\sigma}_{yy}$(a/2, b/2, 0), which produces relatively close results to 3D elasticity bending solutions provided by Zenkour [43].

Zenkour [43] provided 3D exact solutions for exponentially graded rectangular plates under bi-sinusoidal loading. The static analysis was conducted using aluminium (bottom, Al) graded exponentially trough the thickness of a rectangular plate. The following material properties are used for computing the numerical results:

$$E_b = 70 \text{ GPa}, \quad \nu_b = 0.3 \tag{15}$$

The following non-dimensional quantities are used:

$$\bar{w} = w(\frac{a}{2}, \frac{b}{2}, \zeta)\frac{10E_b h^3}{q_0 a^4}, \qquad \bar{\sigma}_{yy} = \sigma_{yy}(\frac{a}{2}, \frac{b}{2}, \zeta)\frac{h^2}{q_0 a^2}, \qquad \bar{\sigma}_{xz} = \tau_{xz}(0, \frac{b}{2}, \zeta)\frac{h}{q_0 a},$$

$$\bar{\zeta} = \frac{\zeta}{h}. \tag{16a-g}$$

Figure 2 shows the exponential function V($\bar{\zeta}$) along the thickness of an EG plate for different values of the parameter *p*.

Firstly, the well-known trigonometric HSDT (HSDT1, see Table 1) which was also studied in Ref. [32] is presented in this paper. This theory, also called trigonometric plate theory (TPT), includes the sine function and it was originally developed by Levy [48], corroborated and improved by Stein [49], extensively used by Touratier [50], Vidal and

Polit [51-54], and recently adapted to functionally graded plates (FGP) and EGP by Zenkour [42-43]. Here, the TPT is discussed in detail in the sense that the corresponding shear strain functions "$f(\zeta) = m\sin(\frac{\zeta}{m})$" and "$g(\zeta) = \cos(\frac{\zeta}{n})$" are expressed as a function of "*m"* and "*n"*, respectively, and because they are directly related to the highly coupled differential equations (Equations 7a-f) through the parameters "*y**" and "*q**", then "*m"* and "*n"* are optimized to give close results to 3D solution obtained by Zenkour [43] as stated above. When $m=n=\frac{h}{\pi}$, the TPT is outlined as special case (noticed that when a/h=2 and a=1, the value of *m*=*n*=0.1592), see for example the Datatips in Figures 3 and 4.

Figure 3 shows the variations of non-dimensionalized vertical deflection with the parameter *m* and *n* for a very thick plate after an optimization procedure (several computations of the partial differential equations by changing the parameter *m* and *n*). It can be noticed that closer results to the 3D solution obtained by Zenkour [43] ($\bar{w} = 1.63774$) can be found with values of $m \neq n \neq \frac{h}{\pi}$ (0.1592). The accuracy in the results are more susceptible to change of *n* (transverse shear strain function "$g(\zeta)$") than *m* (inplane shear strain function "$f(\zeta)$").

In Figure 4 the variations of non-dimensionalized inplane normal stresses with the parameter *m* and *n* after the optimization procedure is shown. In this figure it is even more evident the influence of the parameters *m* and *n* in the results. As in the previous figure the value of *m*=*n*≅2=4*h* in a very thick plate (a/h=2, a=1) produces more accurate results ($\bar{\sigma}_{yy} = 0.4435$) to 3D exact solution ($\bar{\sigma}_{yy} = 0.43051$) than in the case when $m=n=0.1592=\frac{h}{\pi}$ ($\bar{\sigma}_{yy} = 0.4679$). In the first case an error around 3% can be noticed, however in the well-known TPT it is about 8.7%, i.e. after the optimization procedure of this theory 5.7% in accurate is gained. Again, the accurate in the results are more susceptible to change of *n* (transverse shear strain function "$g(\zeta)$") than *m* (inplane shear strain function "$f(\zeta)$"). However, as can be noticed, different values of *m* and *n* can be used according the type of application (for example beams), type of requested results

(displacement or stresses) and considering the degree of accuracy that is intended to reach.

Figure 5 shows the variations of non-dimensionalized vertical displacement and normal stresses with parameters "*m*" and "*n*" for an EGP (a/b=1/6, a/h=2 and *p*={0.1, 1.5}) computed by using the HSDT2 (see Table 1). From Figure 5 can be noticed that the *m* and *n* have both the same influence in the accuracy of vertical displacement. However, *n* parameter is more influent in normal stresses results, i.e. the inplane and transverse shear strain shape functions are very important, and so the selection of both *m* and *n* should be performed carefully. Nevertheless, it is still visible a set of values of *m* and *n* in both plots (dark red color) where good accuracy is achieved. The selected values for *m* and *n* are shown in Table 2. They are used for further computations in this paper.

Figure 6 shows the variations of non-dimensionalized vertical displacement and normal stresses with parameters "*m*" and "*n*" for an EGP (a/b=1/6, a/h=2 and *p*={0.1, 1.5}) computed by using the HSDT3 (see Table 1). In this case it is visible that the *m* parameter is more influent in the non-dimezionalized vertical displacement and normal stresses than the parameter *n*. This can perhaps be explained because the Hybrid HSDT, studied in this case, utilize an exponential transverse shear strain shape function "$g(\zeta)$". However, a set of values for *m* and *n* (dark red color) where good accuracy is achieved can be noticed in Figure 6. Again, the selected values for *m* and *n* are presented in Table 2.

Looking at Figures 3-6, in the context of the present generalized hybrid-type quasi-3D HSDT, it can be said that further studies need to be performed for general conclusions regarding the influence of the shear strain shape functions in the accuracy of the results. Because few studies related to the influence of non-polynomial hybrid type shear strain functions in HSDTs were performed, this paper can lead to a new topic of research.

In what follows, numerical results are presented for different aspect ratios (a/b) and several values of the parameter *p*. Table 3 presents results of nondimensionalized centre plate deflection, $\bar{w}$(a/2, b/2, 0), for very thick plates, a/h={2}. In general, the centre deflection, $\bar{w}$, decreases as *p* or *a/h* increase, and also when b/a decreases. For very thick rectangular plate, b/a={1,6}, the HSDT2 (A, $m=\frac{5}{4h}$ and $n=\frac{3}{4h}$), HSDT3 (A, $m=\frac{3}{4h}$

and $n=\frac{3}{4h^2}$), and HSDT3 (B, $m=\frac{5}{4h}$ and $n=\frac{5}{8h^2}$) present the best results among all the rest of HSDT introduced in this paper. These HSDTs have for example an average error (average of the absolute value of each specific error at (a/2,b/2,0), see Equations (17a-c)) for all the values of *p* considered in Table 3 (a/h=2 and b/a=6) of 1.6%, which decreases as b/a decreases.

$$\text{Error}(\%)=\frac{\sum_{i=1}^{6}|E_i|}{6},$$

$$E_i=\frac{\bar{W}^{p}_{present}-\bar{W}^{p}_{exact}}{\bar{W}^{p}_{exact}}100\%,$$

$$p=\{0.1,0.3,0.5,0.7,1,1.5\} \qquad \text{(17a-c)}$$

Results of in-plane normal stress, $\bar{\sigma}_{yy}$ (a/2,b/2,h/2), of square and rectangular thick plate, a/h={2}, are presented in Table 4. The present results are also compared with 3D elasticity solution and other HSDTs above mentioned. The results for the normal stresses, $\bar{\sigma}_{yy}$, increase with both the increase of the parameter, *p*, and the decrease of the aspect ratio, b/a. Likewise, to evaluate the accuracy of the results, the average error was calculated. Based on this analysis it can be concluded that for very thick rectangular plate, a/h={2} and b/a={1,6}, the HSDT1 (A, $m=4h$ and $n=4h$) appear to be the very good choice, however HSDT1 (B, $m=\frac{\pi}{h}$ and $n=\frac{\pi}{h}$) can be also considered. Similar conclusions are valid when a/h=4 for both nondimensionalized maximum deflection and normal stresses. The analysis of accuracy of shows that the HSDT2 (D, $m=n=\frac{\pi}{2h}$) present the higher error among all the HSDTs presented in this paper. This HSDT is attractive for simplicity, but it is not good option in terms of accuracy.

4.2 Functionally graded shells (case problem 1)

The Ren shell geometry is considered in this case problem. The curvature radii are R_1 = 10 m in the ξ_1 direction and $R_2 = \infty$ in the ξ_2 direction. The dimension *b* is equal to 1 m, while the dimension $a = \frac{\pi}{3} R_1$ m. The considered thickness *h* is 2.5 m, 1 m, 0.1 m and 0.01 m, which means a thickness ratio $\frac{R_1}{h}$ equal to 4, 10, 100 and 1000, respectively. The FG shell is subjected to bi-sinusoidal load (r = s = 1), and it is applied at the top. The material is that proposed by Zenkour [42] (see equation 18) with the Young's modulus changing according to Equation (3b).

E_t = 380 GPa, ν_t = 0.3; E_b = 70 GPa, ν_b = 0.3 (18)

In order to study the accuracy of the present quasy-3D HSDTs, the quasi-exact solution provided by Brischetto [55] is used as reference solution. This reference solution is proposed by dividing the Ren shell in 100 mathematical layers with constant properties and considering for each layer a LM4 theory, this solution is indicated as Nml = 100 in Table 5 as originally named by Brischetto and Carrera [56]. This Table considers the transverse displacement, $\overline{w} = w10^{11}$, in z = 0. The comparison is made between the FSDT, several optimized quasi-3D HSDTs (including the polynomial one, HSDT4 with $f(\zeta)=\zeta^3$ and $g(\zeta)=\zeta^2$, which of course cannot be optimized), the refined HSDTs (LM4, LD4, LM2 and LD2) by Brischetto and Carrera [56] and the referential solution (Mml=100) for different thickness ratios $\frac{R_1}{h}$ and two power-law exponent $p=\{1, 4\}$ for the material law.

Looking at the average errors in Table 5, the first impression is that the FSDT produces very large average errors of vertical deflection of Ren shells (>70%), therefore its use is questionable. In order to select an appropriated quasi-3D HSDT a balance between the accuracy and the number of unknowns in the computation (computational cost) should be

performed. This analysis suggest the use of the HSDT1 (B, m=n=$\frac{\pi}{h}$ or A, m=n=4h). Alternatives optimized quais-3D HSDTs can be the HSDT3 (A, $m=\frac{3}{4h}$ and $n=\frac{3}{4h^2}$) and the HSDT2 (C, $m=\frac{3}{4h}$ and $n=\frac{1}{h}$). In addition, the polynomial one (HSDT4) can be also a good choice. It should be remembered that all the proposed and optimized quasi-3D HSDTs have just 6 unknowns. Interesting procedures to obtain accurate theories exists in the literature and most of them do increase the number of unknowns in order to reach certain accuracy. However, this optimization procedure keeps constant the number of unknowns in the displacement.

4.3 Functionally graded shells (case problem 2)

In this example problem, cylindrical shells are also considered. It is important to remark that the bending problem of shells made of FGMs is not easy to find in the literature, it may be because not much attention were given to the static behavior of FGMs compared with the thermomechanical behavior.

The geometric parameters of the shells are as follows: a=0.2 m, R_1=1 m, and θ_0=0.2 rad. The uniform load is q_0=1.0×10^6 N/m^2. In this case the FG shell is subjected to uniform distributed load (r = s = 100), and it is applied at the top. The functionally graded material (Al/ZrO2, aluminum (Al), zirconia (ZrO2),) is that proposed by Zhao et al. [57] (see Equation 19).

E_t = 151 GPa, v_t = 0.3; E_b = 70 GPa, v_b = 0.3 (19)

Table 6 presents the non-dimensional center deflection $\overline{w}=\frac{\overline{w}}{h}$ of several shell geometries. The aforementioned uniformly loaded square Al/ZrO_2 shells with three different thickness ratios R/h=50,100, 200 are used, and the volume fraction exponents are taken as p=0.5, 1, 2. Results reported by Zhao et al. [57] with shear correction factor of K=5/6 (FSDT) were compared with the quasi-3D HSDTs presented in this paper. As

reported by Zhao et al. [57], the displacement increases against the volume fraction exponent *p*. In general, good agreement between the results exist, except for the HSDT2 (Case B) and HSDT3 (Case C) which in somehow is coherent with the general statements and recommendations of the previous case problem.

5. Conclusions

An unavailable generalized hybrid quasi-3D shear deformation theory for the bending analysis of advanced composite shells is presented. Infinite six unknown's hybrid shear deformation theories, in which the stretching effect is included, can be derived by using the present generalized formulation. In this paper new quasi-3D HSDTs for shells (non-polynomial, hybrid and polynomial) are derived by using the present generalized formulation.

In general, by the proper selection of the inplane and transverse shear strain shape function by an optimization procedure, adequate distribution of the transverse shear strains through the plate thickness can be achieved. Thus, the generalized theory complies with tangential stress-free boundary conditions and a correction factor is not required.

After the optimization procedures over the highly coupled partial deferential equations (which are *m* an *n* parameter dependent) were performed, the key conclusions that emerge from the present numerical results can be summarized as follows:

- Infinite six unknowns' hybrid type shear deformation theories with stretching effect included can be derived and solved.
- All the non-polynomial HSDTs should be optimized in order to improve the accuracy of the theory.
- The optimization procedure in all the cases is, in general, beneficial in terms of accuracy of the non-polynomial hybrid type quasi-3D HSDTs.
- It is possible to gain accuracy by keeping the unknowns or DOFs (in FEM) constant.
- There is not unique quasi-3D HSDT which performs well in any particular example problems, i.e. there exists a *problem dependency matter*.

- Benchmark results for the displacement and stresses of exponential graded rectangular plates are obtained, which can be used for the evaluation of other HSDTs and also to compare results obtained by using numerical methods such as the finite element and meshless methods.

Acknowledgment

The author wants to dedicate this work to Franz Williams who pass away during the supervision of my bachelor thesis. I remember their words “Job, family (Cielo and Lizbeth) and thesis is not easy but not impossible”. I also appreciate a lot his bibliographic support on classical composites.

Appendix A: Elasticity theory [45]

$$\varepsilon_1 = \frac{1}{A_1}\left(\frac{\partial \bar{u}}{\partial \xi_1} + \frac{1}{a_2}\frac{\partial a_1}{\partial \xi_2}\bar{v} + \frac{a_1}{R_1}\bar{w}\right),$$

$$\varepsilon_2 = \frac{1}{A_2}\left(\frac{\partial \bar{v}}{\partial \xi_2} + \frac{1}{a_1}\frac{\partial a_2}{\partial \xi_1}\bar{u} + \frac{a_2}{R_2}\bar{w}\right),$$

$$\varepsilon_3 = \frac{\partial \bar{w}}{\partial \xi_3},$$

$$\varepsilon_4 = \frac{1}{A_2}\frac{\partial \bar{w}}{\partial \xi_2} + A_2\frac{\partial}{\partial \xi_3}\left(\frac{\bar{v}}{A_2}\right),$$

$$\varepsilon_5 = \frac{1}{A_1}\frac{\partial \bar{w}}{\partial \xi_1} + A_1\frac{\partial}{\partial \xi_3}\left(\frac{\bar{u}}{A_1}\right),$$

$$\varepsilon_6 = \frac{A_2}{A_1}\frac{\partial}{\partial \xi_1}\left(\frac{\bar{v}}{A_2}\right) + \frac{A_1}{A_2}\frac{\partial}{\partial \xi_2}\left(\frac{\bar{u}}{A_1}\right), \qquad \text{(A1a-f)}$$

where

$$A_1 = \left(1 + \frac{\xi_3}{R_1}\right)a_1, \qquad A_2 = \left(1 + \frac{\xi_3}{R_2}\right)a_2. \qquad \text{(A2a-b)}$$

References

1. S.S. Vel and R.C. Batra. Three-dimensional exact solution for the vibration of functionally graded rectangular plates. J Sound Vib. 2004;272:703-730.
2. M.B. Bever, P.E. Duwez Gradients in Composite Materials. Mater. Sci. Eng. 1972;10:1-8
3. M. Koizumi. The concept of FGM. Ceramic transactions, Funct Grad Mater 1993;34:3-10.
4. V. Birman, L.W. Byrd. Modeling and analysis of functionally graded materials and structures. ASME Appl. Mech. Rev. 2007;60:195-216.
5. J.L. Mantari, A.S. Oktem, Guedes Soares, C. Bending response of functionally graded plates by using a new higher order shear deformation theory. Composite Structures 2012;94:714-723.
6. J.L. Mantari, C. Guedes Soares. Bending analysis of thick exponentially graded plates using a new trigonometric higher order shear deformation theory. Composite Structures 2012;94:1991-2000.
7. J.L. Mantari, C. Guedes Soares. A novel higher-order shear deformation theory with stretching effect for functionally graded plates. Composites: Part B 2013;45:268-281.
8. J.L. Mantari, C. Guedes Soares. Generalized hybrid quasi-3D shear deformation theory for the static analysis of advanced composite plates. Composite Structures 2012;94:2561-2575.
9. J.L. Mantari, C. Guedes Soares. Finite element formulation of a generalized higher order shear deformation theory for advanced composite plates. Composite Structures 2013;96:545-553.
10. D.K. Jha, Kant Tarun, R.K. Singh. A critical review of recent research on functionally graded plates. Composite Structures 2013;96:833-849.
11. J.N. Reddy. Analysis of functionally graded plates. Int J Numer Meth Eng 2000;684:663-84.
12. S.S. Vel and R.C. Batra. Exact Solutions for Thermoelastic Deformations of Functionally Graded Thick Rectangular Plates. AIAA J. 2002;40(7):1421-1433.

13. S.S. Vel and R.C. Batra. Three-dimensional Analysis of Transient Thermal Stresses in Functionally Graded Plates. Int. J. of Solids & Structures 2003;40:7181-7196.
14. Z.Q. Cheng, R.C. Batra. Deflection relationships between the homogeneous Kirchhoff plate theory and different functionally graded plate theories. Arch Mech 2000;52(1):143-158.
15. K.M. Liew, X. Zhao, Y.Y. Lee. Postbuckling responses of functionally graded cylindrical shells under axial compression and thermal loads. Composites: Part B 2012;43:1621-1630.
16. A.H. Sofiyev, N. Kuruoglu. Torsional vibration and buckling of the cylindrical shell with functionally graded coatings surrounded by an elastic medium. Composites: Part B 2013;45:1133-1142.
17. A.H. Sofiyev, N. Kuruoglu. On a problem of the vibration of functionally graded conical shells with mixed boundary conditions. Composites: Part B 2015;70:122-130.
18. A.H. Sofiyev. Influences of shear stresses on the dynamic instability of exponentially graded sandwich cylindrical shells. Composites Part B 2015;77:349-362.
19. A. Deniz. Non-linear stability analysis of truncated conical shell with functionally graded composite coatings in the finite deflection. Composites: Part B 2013;51:318-326.
20. M. Ghannad, G.H. Rahimi, M.Z. Nejad. Elastic analysis of pressurized thick cylindrical shells with variable thickness made of functionally graded materials. Composites: Part B 2013;45:388-396.
21. M. Fraldi, F. Carannante, L. Nunziante. Analytical solutions for n-phase Functionally Graded Material Cylinders under de Saint Venant load conditions: Homogenization and effects of Poisson ratios on the overall stiffness. Composites: Part B 2013;45:1310-1324.
22. F. Tornabene, N. Fantuzzi, M. Bacciocchi. Free vibrations of free-form doubly-curved shells made of functionally graded materials using higher-order equivalent single layer theories. Composites Part B 2014;67:490-509.

23. X. Xie, H. Zheng, G. Jin. Free vibration of four-parameter functionally graded spherical and parabolic shells of revolution with arbitrary boundary conditions. Composites Part B 2015;77:59-73.
24. Y.W. Kim. Free vibration analysis of FGM cylindrical shell partially resting on Pasternak elastic foundation with an oblique edge. Composites: Part B 2015;70:263-276.
25. A. Shooshtari, S. Razavi. Linear and nonlinear free vibration of a multilayered magneto-electro-elastic doubly-curved shell on elastic foundation. Composites Part B(2015), doi:10.1016/j.compositesb.2015.03.070.
26. Y. Qu, X. Long, G. Yuan, G. Meng. An unified formulation for vibration analysis of functionally graded shells of revolution with arbitrary boundary conditions. Composites: Part B 2013;50:381-402.
27. H.T. Thai, S.E. Kim. A review of theories for the modeling and analysis of functionally graded plates and shells. Composite Structures 2015;128:70–86.
28. E. Carrera, S. Brischetto, M. Cinefra, M. Soave. Effects of thickness stretching in functionally graded plates and shells. Composites: Part B 42;2011:123-133.
29. A.M.A. Neves, A.J.M. Ferreira, E. Carrera, C.M.C. Roque, M. Cinefra, R.M.N. Jorge, C.M.M. Soares. Bending of FGM plates by a sinusoidal plate formulation and collocation with radial basis functions. Mechanics Research Communications 2011;38:368-371.
30. A.M.A. Neves, A.J.M. Ferreira, E. Carrera, C.M.C. Roque, M. Cinefra, R.M.N. Jorge, C.M.M. Soares. A quasi-3D sinusoidal shear deformation theory for the static and free vibration analysis of functionally graded plates. Composites: Part B 2012;43:711–725.
31. A.J.M. Ferreira, E. Carrera, M. Cinefra, C.M.C. Roque, O. Polit. Analysis of laminated shells by a sinusoidal shear deformation theory and radial basis functions collocation, accounting for through-the-thickness deformations. Composites: Part B 2011;42:1276-1284.
32. J.L. Mantari, C. Guedes Soares. Optimized sinusoidal higher order shear deformation theory. Composites: Part B 2014;56:126-136.

33. J.L. Mantari, C. Guedes Soares. A trigonometric plate theory with 5-unknows and stretching effect for advanced composite plates. Composite Structures 2014;107:396-405.

34. H.H. Abdelaziz, H.A. Atmane, I. Mechab, L. Boumia, A. Tounsi, A.B.E Abbas. Static Analysis of Functionally Graded Sandwich Plates Using an Efficient and Simple Refined Theory. Chinese Journal of Aeronautics 2011;24:434-448.

35. I. Mechab, B. Mechab, S. Benaissa. Static and dynamic analysis of functionally graded plates using Four-variable refined plate theory by the new function. Composites: Part B 2013;45:748-757.

36. H.T. Thai, S.E. Kim. A simple quasi-3D sinusoidal shear deformation theory for functionally graded plates. Composite Structures 2013;99:172-180.

37. K.P. Soldatos. A transverse shear deformation theory for homogeneous monoclinic plates. Acta Mechanica 1992;94:195-220.

38. E. Carrera. Theories and finite elements for multilayered plates and shells: a unified compact formulation with numerical assessment and benchmarks. Arch. Comput. Meth. Eng. 2003;10:215-296.

39. L. Demasi. ∞^3 Hierarchy plate theories for thick and thin composite plates: The generalized unified formulation. Compos. Struct. 2008;84:256-270.

40. L. Demasi ∞^6 Mixed plate theories based on the generalized unified formulation. Part I: Governing equations. Compos. Struct. 2009;87:1-11.

41. J.L. Mantari, C. Guedes Soares. Analysis of isotropic and multilayered plates and shells by using a generalized higher-order shear deformation theory. Composite Structures 2012;94:2640-2656.

42. A.M. Zenkour. Generalized shear deformation theory for bending analysis of functionally graded plates. Appl. Math. Model. 2006;30:67-84.

43. A.M. Zenkour. Benchmark trigonometric and 3-D elasticity solutions for an exponentially graded thick rectangular plate. Appl. Math. Model. 2007;77:197-214.

44. H. Matsunaga. Free vibration and stability of functionally graded plates according to 2-D higher-order deformation theory. Compos. Struct. 2008;82:256-270.
45. J.N. Reddy. Mechanics of laminated composite plates: theory and analysis (2nd ed.). CRC Press, Boca Raton (FL), 2004.
46. A.S. Oktem, C. Guedes Soares. Boundary discontinuous Fourier solution for plates and doubly curved panels using a higher order theory. Compos: Part B 2011;42:842-850.
47. W.T. Koiter. A consistent first approximation in the general theory of thin elastic shells. In: Proceedings of first symposium on the theory of thin elastic shells. North-Holland, Amsterdam; 1959.
48. M. Levy. Memoire sur la theorie des plaques elastique planes. J. Math. Pures Appl. 1877;30:219-306.
49. M. Stein. Nonlinear theory for plates and shells including the effects of transverse shearing. AIAA 1986;24(9):1537-44.
50. M. Touratier. An efficient standard plate theory. Int J Eng Sci 1991;29(8):901-916.
51. P. Vidal, O. Polit. A family of sinus finite elements for the analysis of rectangular laminated beams. Composite Structures 2008;84:56-72.
52. P. Vidal, O. Polit. Assessment of the refined sinus model for the non-linear analysis of composite beams. Composite Structures 2009;87:370-381.
53. P. Vidal, O. Polit. A sine finite element using a zig-zag function for the analysis of laminated composite beams. Composites: Part B 2011;42:1671-1682.
54. P. Vidal, O. Polit. A refined sinus plate finite element for laminated and sandwich structures under mechanical and thermomechanical loads. Comput. Methods Appl. Mech. Engrg. 2013;253:396-412.
55. S. Brischetto. Classical and mixed multilayered plate/shell models for multifield problems analysis. PhD thesis at DIASP, Politecnico di Torino, Italy, 2009.
56. S. Brischetto, E. Carrera. Classical and mixed theories for bending analysis of functionally graded materials shells. Proceedings of APCOM'07 in conjunction with EPMESC XI, Kyoto, Japan.

57. X. Zhao, Y.Y. Lee, K.M. Liew. Thermoelastic and vibration analysis of functionally graded cylindrical shells. International Journal of Mechanical Sciences 2009;51:694–707.

Table Legends

Table 1. Shear starin shape functions of the hybrid type qusi-3D HSDTs.

Table 2. Selection of the parameter and particularities of the quasi-3D HSDTs.

Table 3. Non-dimensionalized center deflection $\bar{w}$(a/2, b/2, 0) for various EGM rectangular plates, a/h=2.

Table 4. Nondimensionalized normal stresses $\bar{\sigma}_{yy}$(a/2, b/2, h/2) for EGM rectangular plates, a/h=2.

Table 5. Transverse displacement (w = w10^{10}) of FG Ren shell geometry.

Table 6. Non-dimensional center deflections of several shell geometries.

Figure Captions

Figure 1. Geometry of a functionally graded plate

Figure 2. Exponentially graded function V($\bar{\zeta}$) along the thickness of an EG shell for different values of the parameter ‘‘*p*’’.

Figure 3. Variations of non-dimensionalized vertical deflection with parameters “*m*” and “*n*” (HSDT1, a/b=1/6, a/h=2 and *p*=0.1).

Figure 4. Variations of non-dimensionalized inplane normal stresses with parameters “*m*” and “*n*” (HSDT1, a/b=1/6, a/h=2 and p=1.5).

Figure 5. Variations of non-dimensionalized vertical displacement and inplane normal stresses with parameters “*m*” and “*n*” (HSDT2, a/b=1/6, a/h=2 and *p*={0.1, 1.5}).

Figure 6. Variations of non-dimensionalized vertical displacement and inplane normal stresses with parameters "*m*" and "*n*" (HSDT3, a/b=1/6, a/h=2 and *p*={0.1, 1.5}).

Tables

Table 1.

Model	*f(ζ)* and *g(ζ)* function	Particularities
Present trigonometric HSDT(HSDT1)	$f(\zeta)=m\sin(\frac{\zeta}{m})$ $g(\zeta)=\cos(\frac{\zeta}{n})$	$y^*=-\cos(\frac{h}{2m})$ $q^*=-\cos(\frac{h}{2n})$
Present trigonometric HSDT(HSDT2)	$f(\zeta)=\tan(m\zeta)$ $g(\zeta)=\sec(n\zeta)$	$y^*=-m\sec^2(\frac{mh}{2})$ $q^*=-\sec(\frac{nh}{2})$
Present hybrid HSDT(HSDT3)	$f(\zeta)=\tan(m\zeta)$ $g(\zeta)=e^{n\zeta^2}$	$y^*=-m\sec^2(\frac{mh}{2})$ $q^*=-e^{nh^2/4}$
Present hybrid HSDT(HSDT3)	$f(\zeta)=\zeta^3$ $g(\zeta)=\zeta^2$	$y^*=-\frac{3h^2}{4}$, $q^*=-\frac{h^2}{4}$

Table 2.

Optimized HSDT	Option	m and n	y^* and q^*
Present trigonometric HSDT(HSDT1)	A	$m=4h,\ n=4h$	$y^*=-\cos(\frac{1}{8}),\ q^*=-\cos(\frac{1}{8})$
	B	$m=\frac{h}{\pi},\ n=\frac{h}{\pi}$	$y^*=0,\ q^*=0$
Present trigonometric HSDT(HSDT2)	A	$m=\frac{5}{4h},\ n=\frac{3}{4h}$	$y^*=-\frac{5}{4h}\sec^2(\frac{5}{8}),\ q^*=-\sec(\frac{3}{8})$
	B	$m=\frac{1}{5h},\ n=\frac{1}{2h}$	$y^*=-\frac{1}{5h}\sec^2(\frac{1}{10}),\ q^*=-\sec(\frac{1}{4})$
	C	$m=\frac{3}{4h},\ n=\frac{1}{h}$	$y^*=-\frac{3}{4h}\sec^2(\frac{3}{8}),\ q^*=-\sec(\frac{1}{2})$
	D	$m=\frac{\pi}{2h},\ n=\frac{\pi}{2h}$	$y^*=-\frac{\pi}{h},\ q^*=-\sqrt{2}$
Present hybrid HSDT(HSDT3)	A	$m=\frac{3}{4h},\ n=\frac{3}{4h^2}$	$y^*=-\frac{3}{4h}\sec^2(\frac{3}{8}),\ q^*=-e^{-\frac{3}{16}}$
	B	$m=\frac{5}{4h},\ n=\frac{5}{8h^2}$	$y^*=-\frac{5}{4h}\sec^2(\frac{5}{8}),\ q^*=-e^{-\frac{5}{32}}$
	C	$m=\frac{1}{5h},\ n=\frac{3}{8h^2}$	$y^*=-\frac{1}{5h}\sec^2(\frac{1}{10}),\ q^*=-e^{-\frac{3}{32}}$
Present hybrid HSDT(HSDT4)	NA	NA	$y^*=-\frac{3h^2}{4},\ q^*=-\frac{h^2}{4}$

NA: No applicable

Table 3.

a/h	b/a	Theory	p=0.1	diff.	p=0.3	diff.	p=0.5	diff.	p=0.7	diff.	p=1.0	diff.	p=1.5	diff.	Avrg.
2	6	**3-D[43]**	**1.63774**	**(%)**	**1.48846**	**(%)**	**1.35184**	**(%)**	**1.22688**	**(%)**	**1.05929**	**(%)**	**0.82606**	**(%)**	**(%)**
		Present (HSDT1) A	1.63627	-0.1	1.47929	-0.6	1.33623	-1.2	1.20598	-1.7	1.03245	-2.5	0.79371	-3.9	1.7
		Present (HSDT1) B	1.62939	-0.5	1.47309	-1.0	1.33066	-1.6	1.20101	-2.1	1.02823	-2.9	0.79056	-4.3	2.1
		Present (HSDT2) A	1.63704	0.0	1.47995	-0.6	1.33677	-1.1	1.20639	-1.7	1.03263	-2.5	0.79359	-3.9	1.6
		Present (HSDT2) B	1.63661	-0.1	1.47960	-0.6	1.33651	-1.1	1.20624	-1.7	1.03624	-2.2	0.77894	-5.7	1.9
		Present (HSDT2) C	1.63756	0.0	1.48046	-0.5	1.33730	-1.1	1.20690	-1.6	1.03323	-2.5	0.79429	-3.8	1.6
		Present (HSDT2) D	1.63518	-0.2	1.47828	-0.7	1.33526	-1.2	1.20504	-1.8	1.03150	-2.6	0.79277	-4.0	1.8
		Present (HSDT3) A	1.63748	0.0	1.48038	-0.5	1.33723	-1.1	1.20683	-1.6	1.03316	-2.5	0.79422	-3.9	1.6
		Present (HSDT3) B	1.63712	0.0	1.48002	-0.6	1.33684	-1.1	1.20646	-1.7	1.03270	-2.5	0.79366	-3.9	1.6
		Present (HSDT3) C	1.63684	-0.1	1.47982	-0.6	1.33667	-1.1	1.20638	-1.7	1.03635	-2.2	0.77905	-5.7	1.9
		Present (HSDT4)	1.63629	-0.1	1.47931	-0.6	1.33625	-1.2	1.20601	-1.7	1.03244	-2.5	0.79369	-3.9	1.7
		quasi-3D HSDT [7]	1.63654	-0.1	1.47953	-0.6	1.33644	-1.1	1.20618	-1.7	1.03325	-2.5	0.79387	-3.9	1.6
	1	**3-D[43]**	**0.57693**		**0.52473**		**0.47664**		**0.43240**		**0.37269**		**0.28904**		
		Present (HSDT1) A	0.57761	0.1	0.52215	-0.5	0.47156	-1.1	0.42547	-1.6	0.36400	-2.3	0.27925	-3.4	1.5
		Present (HSDT1) B	0.57308	-0.7	0.51806	-1.3	0.46788	-1.8	0.42216	-2.4	0.36117	-3.1	0.27712	-4.1	2.2
		Present (HSDT2) A	0.57915	0.4	0.52352	-0.2	0.47278	-0.8	0.42652	-1.4	0.36481	-2.1	0.27973	-3.2	1.4
		Present (HSDT2) B	0.57797	0.2	0.52247	-0.4	0.47186	-1.0	0.42574	-1.5	0.36798	-1.3	0.26509	-8.3	2.1
		Present (HSDT2) C	0.57937	0.4	0.52375	-0.2	0.47302	-0.8	0.42672	-1.3	0.36506	-2.0	0.28002	-3.1	1.3
		Present (HSDT2) D	0.58111	0.7	0.52529	0.1	0.47435	-0.5	0.42793	-1.0	0.36598	-1.8	0.28057	-2.9	1.2
		Present (HSDT3) A	0.57919	0.4	0.52359	-0.2	0.47287	-0.8	0.42659	-1.3	0.36494	-2.1	0.27993	-3.2	1.3
		Present (HSDT3) B	0.57933	0.4	0.52369	-0.2	0.47292	-0.8	0.42666	-1.3	0.36493	-2.1	0.27983	-3.2	1.3
		Present (HSDT3) C	0.57822	0.2	0.52270	-0.4	0.47205	-1.0	0.42591	-1.5	0.36812	-1.2	0.26519	-8.3	2.1
		Present (HSDT4)	0.57763	0.1	0.52217	-0.5	0.47158	-1.1	0.42549	-1.6	0.36400	-2.3	0.27924	-3.4	1.5
		quasi-3D HSDT [7]	0.57789	0.2	0.52240	-0.4	0.47179	-1.0	0.42567	-1.6	0.36485	-2.1	0.27939	-3.3	1.4

Table 4.

a/h	b/a	Theory	p=0.1	diff.	p=0.3	diff.	p=0.5	diff.	p=0.7	diff.	p=1.0	diff.	p=1.5	diff.	Avrg.
2	6	**3-D[43]**	**0.2943**	**(%)**	**0.3101**	**(%)**	**0.3270**	**(%)**	**0.3451**	**(%)**	**0.3746**	**(%)**	**0.4305**	**(%)**	**(%)**
		Present (HSDT1) A	0.2773	-5.8	0.2966	-4.4	0.3171	-3.0	0.3391	-1.7	0.3750	0.1	0.4435	3.0	3.0
		Present (HSDT1) B	0.2912	-1.1	0.3118	0.6	0.3339	2.1	0.3573	3.5	0.3955	5.6	0.4679	8.7	3.6
		Present (HSDT2) A	0.2711	-7.9	0.2897	-6.6	0.3096	-5.3	0.3309	-4.1	0.3657	-2.4	0.4322	0.4	4.4
		Present (HSDT2) B	0.2758	-6.3	0.2949	-4.9	0.3153	-3.6	0.3371	-2.3	0.3740	-0.2	0.4325	0.5	2.9
		Present (HSDT2) C	0.2703	-8.1	0.2889	-6.8	0.3088	-5.6	0.3300	-4.4	0.3648	-2.6	0.4312	0.2	4.6
		Present (HSDT2) D	0.2559	-13.0	0.2730	-11.9	0.2914	-10.9	0.3111	-9.9	0.3434	-8.3	0.4054	-5.8	10.0
		Present (HSDT3) A	0.2713	-7.8	0.2900	-6.5	0.3100	-5.2	0.3313	-4.0	0.3662	-2.2	0.4329	0.6	4.4
		Present (HSDT3) B	0.2702	-8.2	0.2887	-6.9	0.3085	-5.6	0.3298	-4.4	0.3644	-2.7	0.4306	0.0	4.7
		Present (HSDT3) C	0.2747	-6.7	0.2937	-5.3	0.3140	-4.0	0.3357	-2.7	0.3725	-0.6	0.4305	0.0	3.2
		Present (HSDT4)	0.2772	-5.8	0.2965	-4.4	0.3171	-3.0	0.3390	-1.8	0.3749	0.1	0.4433	3.0	3.0
		quasi-3D HSDT [7]	0.2763	-6.1	0.2954	-4.7	0.3159	-3.4	0.3378	-2.1	0.3737	-0.2	0.4416	2.6	3.2
	1	**3-D[43]**	**0.3103**		**0.3292**		**0.3495**		**0.3713**		**0.4068**		**0.4741**		
		Present (HSDT1) A	0.2927	-5.7	0.3149	-4.3	0.3386	-3.1	0.3636	-2.1	0.4039	-0.7	0.4790	1.0	2.8
		Present (HSDT1) B	0.2955	-4.8	0.3181	-3.4	0.3421	-2.1	0.3675	-1.0	0.4085	0.4	0.4851	2.3	2.3
		Present (HSDT2) A	0.2879	-7.2	0.3096	-6.0	0.3327	-4.8	0.3571	-3.8	0.3965	-2.5	0.4698	-0.9	4.2
		Present (HSDT2) B	0.2926	-5.7	0.3149	-4.4	0.3385	-3.2	0.3635	-2.1	0.4067	0.0	0.4609	-2.8	3.0
		Present (HSDT2) C	0.2912	-6.2	0.3133	-4.8	0.3368	-3.6	0.3616	-2.6	0.4015	-1.3	0.4758	0.4	3.2
		Present (HSDT2) D	0.2847	-8.3	0.3061	-7.0	0.3288	-5.9	0.3528	-5.0	0.3913	-3.8	0.4628	-2.4	5.4
		Present (HSDT3) A	0.2912	-6.2	0.3133	-4.8	0.3368	-3.7	0.3615	-2.6	0.4015	-1.3	0.4759	0.4	3.2
		Present (HSDT3) B	0.2879	-7.2	0.3097	-5.9	0.3327	-4.8	0.3572	-3.8	0.3965	-2.5	0.4698	-0.9	4.2
		Present (HSDT3) C	0.2926	-5.7	0.3149	-4.4	0.3385	-3.2	0.3635	-2.1	0.4067	0.0	0.4607	-2.8	3.0
		Present (HSDT4)	0.2927	-5.7	0.3149	-4.3	0.3385	-3.1	0.3636	-2.1	0.4039	-0.7	0.4790	1.0	2.8
		quasi-3D HSDT [7]	0.2924	-5.8	0.3147	-4.4	0.3383	-3.2	0.3633	-2.2	0.4040	-0.7	0.4785	0.9	2.9

Table 5.

w(0)										
p	**Theory \ R1/h**	**4**	**diff.(%)**	**10**	**diff.(%)**	**100**	**diff.(%)**	**1000**	**diff.(%)**	**Avrg.(%)**
1	Nml=100	0.018		0.170		52.781		4201.3		
	LM4	0.013	-27.8	0.170	0.0	52.783	0.0	4201.4	0.0	-9.3
	LD4	0.013	-27.8	0.170	0.0	52.783	0.0	4201.4	0.0	-9.3
	LM2	0.013	-27.8	0.162	-4.7	52.693	-0.2	4201.4	0.0	-10.9
	LD2	0.014	-22.2	0.162	-4.7	52.692	-0.2	4201.4	0.0	-9.0
	FSDT	0.054	200.0	0.170	0.0	43.735	-17.1	3792.2	-9.7	61.0
	Present (HSDT1) A	0.015	-14.6	0.162	-4.6	52.263	-1.0	3978.1	-5.3	-6.7
	Present (HSDT1) B	0.011	-41.1	0.159	-6.3	52.109	-1.3	3975.2	-5.4	-16.2
	Present (HSDT2) A	0.018	-2.2	0.164	-3.7	52.251	-1.0	3977.9	-5.3	-2.3
	Present (HSDT2) B	0.016	-11.7	0.163	-4.4	52.261	-1.0	3978.1	-5.3	-5.7
	Present (HSDT2) C	0.018	-1.1	0.164	-3.8	52.228	-1.0	3977.4	-5.3	-2.0
	Present (HSDT2) D	0.023	26.7	0.166	-2.4	52.015	-1.5	3973.5	-5.4	7.6
	Present (HSDT3) A	0.018	-2.8	0.164	-3.8	52.237	-1.0	3977.6	-5.3	-2.5
	Present (HSDT3) B	0.018	0.0	0.164	-3.6	52.243	-1.0	3977.8	-5.3	-1.6
	Present (HSDT3) C	0.016	-9.4	0.163	-4.3	52.257	-1.0	3978.0	-5.3	-4.9
	Present (HSDT4)	0.015	-14.4	0.162	-4.5	52.263	-1.0	3978.1	-5.3	-6.7
4	Nml=100	0.032		0.314		79.739		7081.1		
	LM4	0.022	-31.3	0.315	0.3	79.734	0.0	7081.6	0.0	-10.3
	LD4	0.021	-34.4	0.315	0.3	79.734	0.0	7081.6	0.0	-11.4
	LM2	0.028	-12.5	0.287	-8.6	79.345	-0.5	7081.6	0.0	-7.2
	LD2	0.032	0.0	0.288	-8.3	79.344	-0.5	7081.6	0.0	-2.9
	FSDT	0.090	181.3	0.277	-11.8	65.603	-17.7	6384.2	-9.8	50.6
	Present (HSDT1) A	0.040	24.4	0.308	-1.9	78.236	-1.9	6780.3	-4.2	6.9
	Present (HSDT1) B	0.030	-5.6	0.303	-3.6	78.016	-2.2	6776.6	-4.3	-3.8
	Present (HSDT2) A	0.045	39.1	0.310	-1.4	78.203	-1.9	6779.3	-4.3	11.9
	Present (HSDT2) B	0.041	27.5	0.308	-1.8	78.240	-1.9	6779.9	-4.3	7.9
	Present (HSDT2) C	0.051	60.3	0.310	-1.3	78.197	-1.9	6777.9	-4.3	19.0
	Present (HSDT2) D	0.054	67.5	0.312	-0.6	77.911	-2.3	6768.8	-4.4	21.5
	Present (HSDT3) A	0.051	58.4	0.310	-1.4	78.207	-1.9	6778.4	-4.3	18.4
	Present (HSDT3) B	0.045	40.9	0.310	-1.3	78.196	-1.9	6778.9	-4.3	12.6
	Present (HSDT3) C	0.042	29.7	0.309	-1.7	78.229	-1.9	6779.6	-4.3	8.7
	Present (HSDT4)	0.040	24.7	0.308	-1.9	78.236	-1.9	6780.2	-4.2	7.0

Table 6.

p	w(0)			
	Theory	R1/h		
		50	100	200
0.5	Ref. [57]	0.0038	0.0543	0.6503
	Present (HSDT1) A	0.0038	0.0544	0.6411
	Present (HSDT1) B	0.0038	0.0542	0.6399
	Present (HSDT2) A	0.0038	0.0543	0.6410
	Present (HSDT2) B	0.0034	0.0538	0.6402
	Present (HSDT2) C	0.0038	0.0543	0.6408
	Present (HSDT2) D	0.0038	0.0541	0.6391
	Present (HSDT3) A	0.0038	0.0543	0.6409
	Present (HSDT3) B	0.0038	0.0543	0.6409
	Present (HSDT3) C	0.0034	0.0538	0.6402
	Present (HSDT4)	0.0038	0.0544	0.6415
1	Ref. [57]	0.0043	0.0607	0.7283
	Present (HSDT1) A	0.0043	0.0608	0.7204
	Present (HSDT1) B	0.0043	0.0606	0.7186
	Present (HSDT2) A	0.0043	0.0608	0.7203
	Present (HSDT2) B	0.0043	0.0608	0.7204
	Present (HSDT2) C	0.0043	0.0608	0.7200
	Present (HSDT2) D	0.0042	0.0605	0.7176
	Present (HSDT3) A	0.0043	0.0608	0.7201
	Present (HSDT3) B	0.0043	0.0608	0.7202
	Present (HSDT3) C	0.0043	0.0608	0.7203
	Present (HSDT4)	0.0043	0.0608	0.7204
2	Ref. [57]	0.0047	0.0666	0.8057
	Present (HSDT1) A	0.0047	0.0667	0.7991
	Present (HSDT1) B	0.0047	0.0665	0.7971
	Present (HSDT2) A	0.0047	0.0667	0.7989
	Present (HSDT2) B	0.0047	0.0667	0.7990
	Present (HSDT2) C	0.0047	0.0667	0.7986
	Present (HSDT2) D	0.0047	0.0664	0.7958
	Present (HSDT3) A	0.0047	0.0667	0.7987
	Present (HSDT3) B	0.0047	0.0667	0.7988
	Present (HSDT3) C	0.0047	0.0667	0.7990
	Present (HSDT4)	0.0047	0.0667	0.7991

Figures

Fig. 1

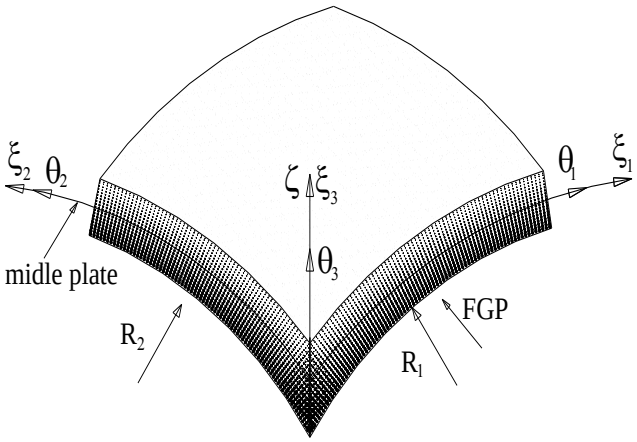

Fig. 2

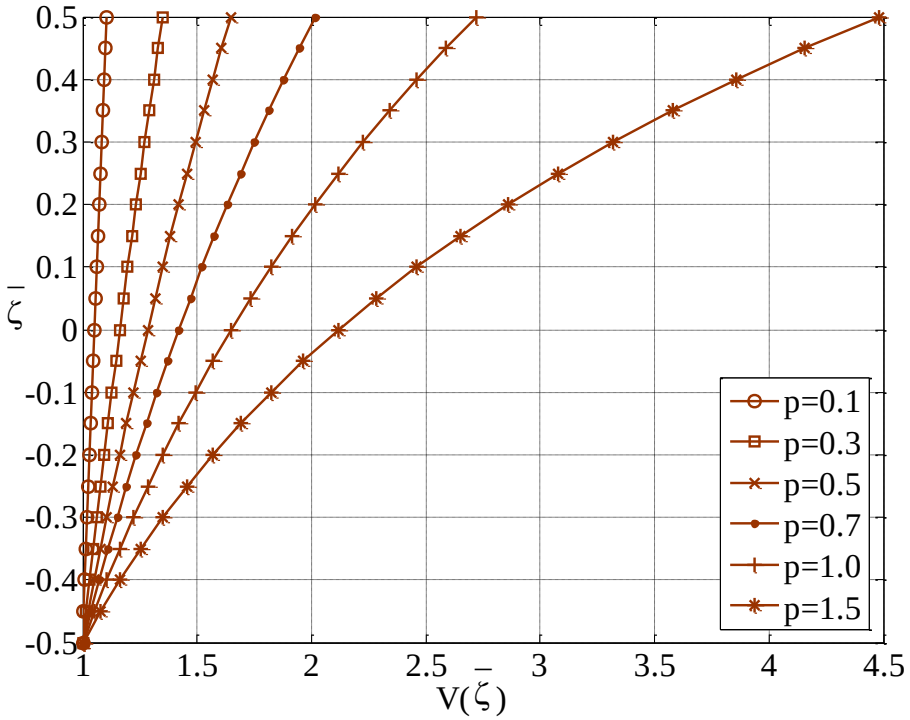

Fig. 3

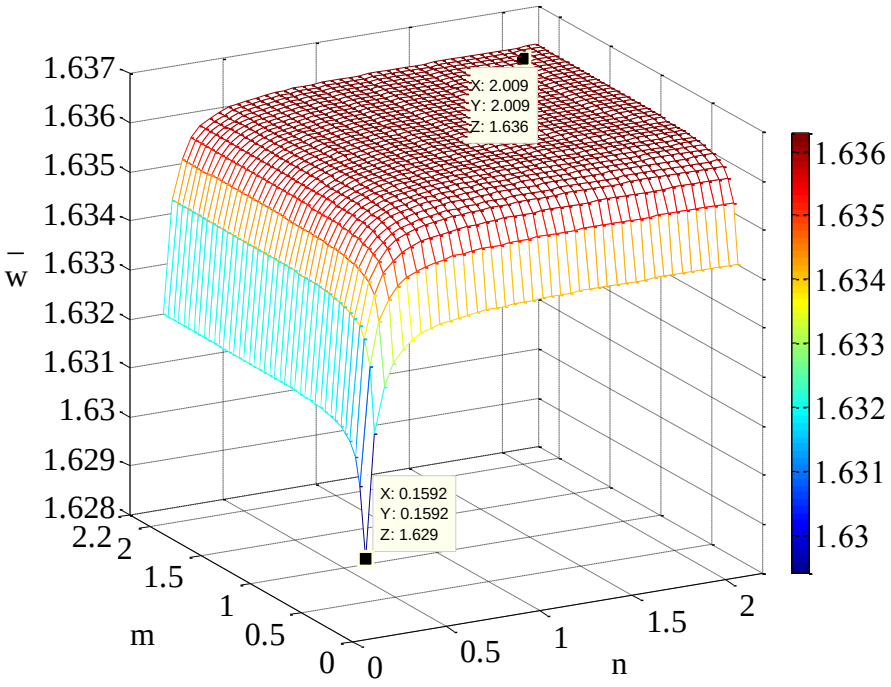
1.637
1.636
1.635
1.634
1.633
1.632
1.631
1.63
1.629
1.628
$\bar{w}$
X: 2.009
Y: 2.009
Z: 1.636
X: 0.1592
Y: 0.1592
Z: 1.629
2.2
2
1.5
1
0.5
0
m
0
0.5
1
1.5
2
n
1.636
1.635
1.634
1.633
1.632
1.631
1.63

Fig. 4

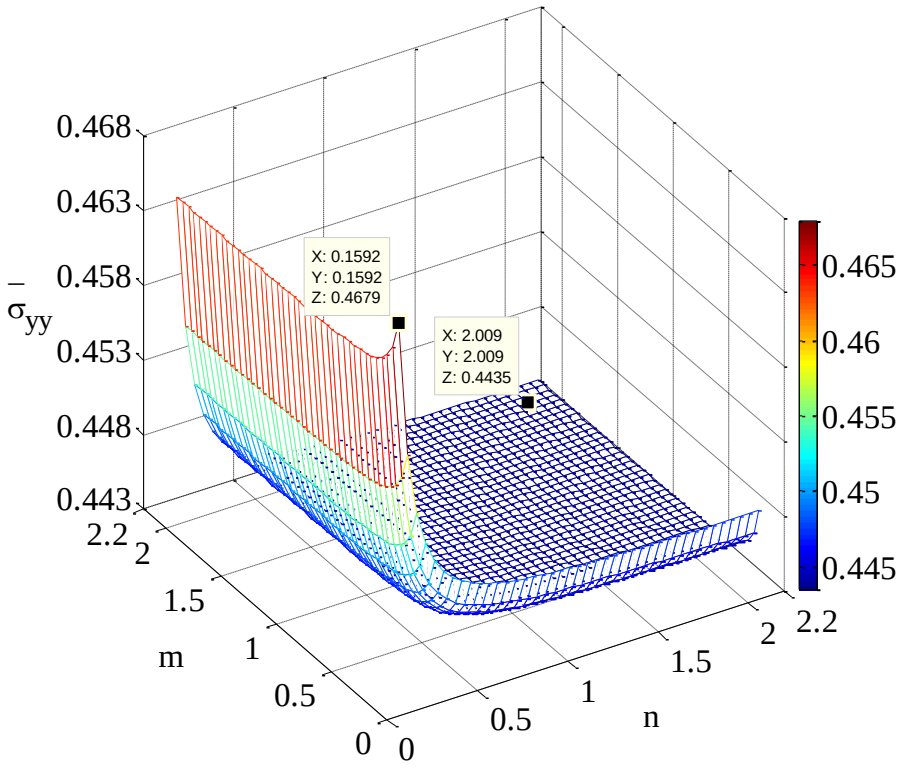
0.468
0.463
0.458
0.453
0.448
0.443
$\bar{\sigma}_{yy}$
X: 0.1592
Y: 0.1592
Z: 0.4679
X: 2.009
Y: 2.009
Z: 0.4435
2.2
2
1.5
1
0.5
0
m
0
0.5
1
1.5
2
2.2
n
0.465
0.46
0.455
0.45
0.445

Fig. 5

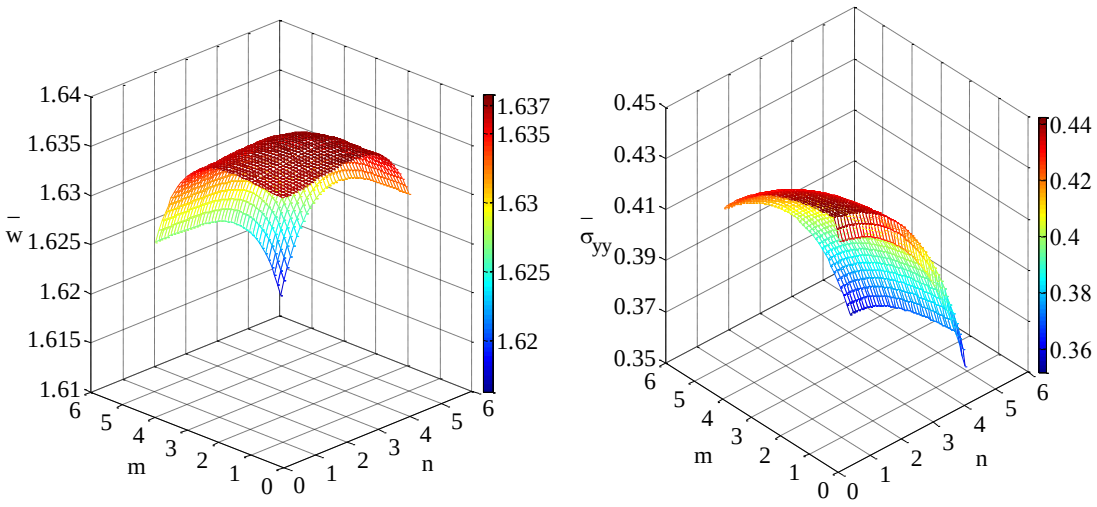
$\bar{w}$
1.64
1.635
1.63
1.625
1.62
1.615
1.61
1.637
1.635
1.63
1.625
1.62
m
n
$\bar{\sigma}_{yy}$
0.45
0.43
0.41
0.39
0.37
0.35
0.44
0.42
0.4
0.38
0.36

Fig. 6

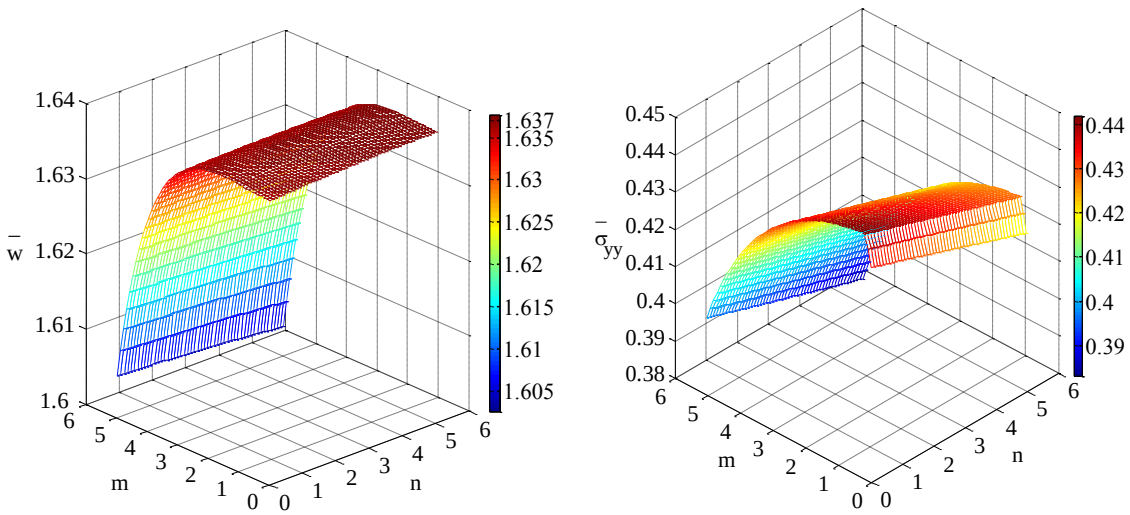
$\bar{w}$
1.64
1.63
1.62
1.61
1.6
1.637
1.635
1.63
1.625
1.62
1.615
1.61
1.605
m
n
$\bar{\sigma}_{yy}$
0.45
0.44
0.43
0.42
0.41
0.4
0.39
0.38
0.44
0.43
0.42
0.41
0.4
0.39